Correlation of structure and dielectric properties of silver selenomolybdate glasses

B. Deb and A. Ghosh

Related Articles

Additional information on J. Appl. Phys.

Journal Homepage: http://jap.aip.org/
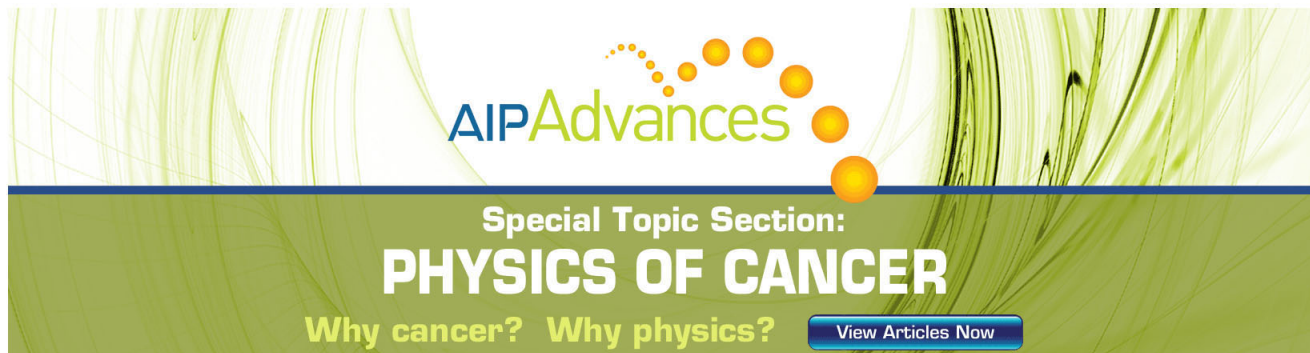
Journal Information: http://jap.aip.org/about/about_the_journal

Top downloads: http://jap.aip.org/features/most_downloaded

Information for Authors: http://jap.aip.org/authors

Correlation of structure and dielectric properties of silver selenomolybdate glasses

B. Deb[a)] and A. Ghosh[b)]
Department of Solid State Physics, Indian Association for the Cultivation of Science, Jadavpur, Kolkata 700032, India

Structure and dielectric properties of the glasses of compositions yAg_2O-(1-y)$(xSeO_2$-(1-x)$MoO_3)$ with varying modifier oxide and glass formers ratio have been reported in this paper. Fourier transform infrared (FTIR) spectroscopy has been employed to investigate the effect of SeO_2 content on the glass network structure. The existence of different characteristic absorption bands corresponding to the vibration of SeO_3^{2-} anions, isolated MoO_6 units and crystalline molybdate octahedra, has been ascertained from FTIR spectra. It has been observed that the modification of the glass network structure occurs with change of SeO_2 content, which reveals the dual role of SeO_2 as a network modifier and a network former depending on composition. The dielectric constant as well as dielectric strength increases gradually with the increase of SeO_2 content for low modifier oxide content (y), whereas they show a maximum for intermediate and highly modified glasses. The variation of the dielectric parameters correlates directly to the relative proportion of vibration mode of SeO_3^{2-} ions, which is observed to vary in a similar fashion to dielectric parameters and is, thus in turn, related to the dual behavior of SeO_2 as a modifier and a former depending on composition. © *2012 American Institute of Physics*. [http://dx.doi.org/10.1063/1.4737259]

I. INTRODUCTION

Ion conducting glasses have engrossed a major research thrust due to their potential application in solid state electrochemical devices, sensors etc.[1–5] But the designing of ionic glasses for technological application is difficult due to their complex disorder structure.[6–9] The structure and ion transport properties[10–13] of glass systems containing modifier oxide like Ag_2O, Li_2O, etc. and network formers like B_2O_3, P_2O_5, etc. have been reported. SeO_2 is a non-traditional network former and cannot easily form glass. However, it has been revealed in recent years that it is indeed possible to obtain different multicomponent selenite glasses when additional network forming oxides are present.[14,15]

Glasses containing more than one network former is interesting from scientific as well as technological point of view to understand the influence of the simultaneous presence of different network formers on microscopic and macroscopic glass properties such as glass structure, thermal property, dielectric properties, electrical properties etc.[16–20] Glass formation based on the network former SeO_2 and other network formers like TeO_2, V_2O_5, MoO_3 has been reported recently.[14,21,22] It is observed that in Ag_2O-SeO_2-B_2O_3 and Ag_2O-SeO_2-MoO_3 glasses the glass formation mainly lies towards SeO_2 end.[22] The addition of SeO_2 in these glasses forms mostly to the mixed Se–O– types bonds during the amorphous network formation.[22] In most of these glasses formation, participation of isolated SeO_3 units in the glass structure is confirmed.[21] The IR study of a few Ag_2SeO_3-MoO_3 glasses reveals new interesting results on the role of MoO_3 in the modification of glass structure.[23] The existence of different structural units of MoO_4, MoO_6, and SeO_3 groups is confirmed in such glasses.[23] The increase in the MoO_3 content leads to the increase in the MoO_6 network units which is connected by bridging Mo–O–Mo bonds. Recently, in a few Li_2O modified SeO_2 based glasses the study of Se K-edge EXAFS/XANES reveals the local coordination environment of selenium.[24,25] It is observed that the coordination of selenium changes from 4 to 3 which are attributed to the conversion of oxygen rich selenate phase to oxygen deficit selenite phase with increase of SeO_2 content in the glass composition and consequently affecting the network structure.[25] This decrease in turn indicates that size of Se-O clusters increases as the SeO_2 content increases in the glass composition. The modification of the network structure occurs from layers to chains with increasing SeO_2 content. The modification of network structure from layer to chain or more complex dimension depends on the nature of additional network formers. At low SeO_2 content, the SeO_2 gets dissolved in the network structure; whereas at high content, the network forming tendency increases.[25] The glass formation of different selenite compounds is thus related to the creation of disorder in the SeO_3 chains by the modifier polyhedra at a suitable compositional ratio. The understanding of glass formation in glass systems containing multiple non-traditional glass network formers and its consequent effect on glass structure, physical, optical, and other properties thus elicits an important scientific challenge.

The relaxation data of materials can be expressed in various ways, using different representations such as in complex dielectric permittivity formalism or in complex electric modulus formalism. The dielectric constant, dielectric strength, and the dissipation factor obtained from dielectric study can reveal the origin of dielectric dispersion and relevant

a)Present address: Department of Physics, Govt. Degree College, Dharmanagar, Tripura – 799250.
b)Author to whom correspondence should be addressed. Electronic mail: sspag@iacs.res.in.

relaxation phenomena.[26] Based on values of the activation energy and the characteristic relaxation time, it is possible to determine the different relaxation processes.

In this paper, we have studied the structure and dielectric constants of Ag_2O-SeO_2-MoO_3 glass system containing non-traditional glass network formers of varying ratio. The effect of variation of modifier oxide (Ag_2O) as well as the network formers ratio on the glass structure and on the dielectric property was investigated. The values of dielectric constant, dielectric strength, and electrode polarization relaxation time were obtained and correlated to the change of the glass network structure.

II. EXPERIMENTAL DETAILS

Glass samples of compositions yAg_2O-$(1-y)(xSeO_2$-$(1-x)MoO_3)$ where $x = 0.40$, 0.50, 0.60, 0.70, and 0.80 and $y = 0.20$, 0.30, and 0.40 were prepared by melt quenching techniques. Appropriate amounts of $AgNO_3$, SeO_2, and MoO_3 were mixed and preheated in an alumina crucible at $400\,^{\circ}C$ for 2 hours for denitrogenation of $AgNO_3$. The mixtures were then melted in the temperature range 550–$650\,^{\circ}C$ depending on composition and equilibrated for 1 hour. The melts were then rapidly quenched between two aluminum plates to obtain the desired glass samples.

The glass formation was confirmed from the x-ray diffraction studies of the samples. The FTIR spectra of the powder samples in KBr matrix in the ratio 1:100 were recorded at room temperature using a FTIR spectrometer (PerkinElmer, model Spectrum100). The dielectric data of the samples were measured using an LCR meter (Quad Tech, model 7600) in the frequency range of 10 Hz-2 MHz and in a wide temperature range.

III. RESULTS AND DISCUSSION

A. FTIR spectra

The FTIR spectra for several glass samples are shown in Figs. 1(a) and 1(b). The spectra show different absorption bands corresponding to characteristic vibration modes present in the glasses. The major absorption bands are observed at $\sim 500\,cm^{-1}$, ~ 600–$610\,cm^{-1}$, ~ 700–$720\,cm^{-1}$, ~ 760–$780\,cm^{-1}$, ~ 860–$870\,cm^{-1}$, and ~ 890–$910\,cm^{-1}$. The band at $500\,cm^{-1}$ is due to the vibration of Se-O bond present in SeO_3 units.[21] The bands centered at ~ 700–$720\,cm^{-1}$, 760–$780\,cm^{-1}$, and 860–$870\,cm^{-1}$ are assigned to the vibration of SeO_3^{2-} selenite ion.[21–23] The band at 600–$610\,cm^{-1}$ is assigned to the vibration of isolated MoO_6 units, and the band at 890–$900\,cm^{-1}$ is attributed to the vibration of Mo_2O_8 molybdate octahedral units.[23,27]

It is noted that for $y = 0.20$ series (Fig. 1(a)), the band position corresponding to $500\,cm^{-1}$, 600–$610\,cm^{-1}$, and 700–$720\,cm^{-1}$ remains almost unaltered with change of glass formers ratio but the intensity changes slightly. The band positions centered at ~ 760–$780\,cm^{-1}$ and ~ 860–$870\,cm^{-1}$ shift towards higher wave number with increase of SeO_2 content whereas that at ~ 890–$910\,cm^{-1}$ slightly shifts towards lower wave number. Thus, the vibration due to SeO_3^{2-} ion becomes
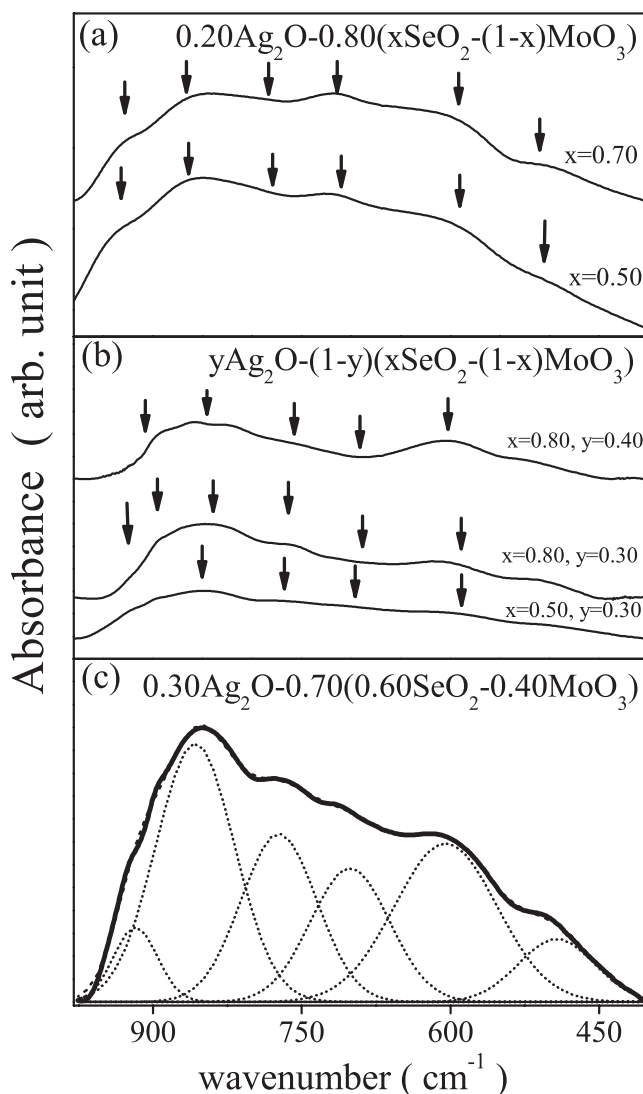

FIG. 1. FTIR spectra for the (a) glasses of composition $0.20Ag_2O$-$0.80(xSeO_2$-$(1-x)MoO_3)$ and (b) for several glasses of compositions yAg_2O-$(1-y)(xSeO_2$-$(1-x)MoO_3)$. Arrows indicate the position of absorption bands. Panel (c) shows deconvolution of a selected FTIR spectrum.

prominent with the increase of SeO_2 whereas that of isolated molybdate units decreases.

For $y = 0.30$ series (see Fig. 1(b)), the band at ~ 600–$610\,cm^{-1}$ shifts slightly towards higher wave number at higher SeO_2 content, whereas that at ~ 890–$910\,cm^{-1}$ remains almost unaltered. The band position at 860–$870\,cm^{-1}$ shows a gradual shift towards higher wave number with increase of SeO_2 content. The other bands position shows similar behavior as that observed for $y = 0.20$ series.

For $y = 0.40$ series (see Fig. 1(b)), the FTIR spectra are quite different from that of $y = 0.20$ and $y = 0.30$ series. Here, the intensity of the characteristic vibration modes is significantly enhanced. This indicates that increasing Ag_2O content also affects and possibly alters the glass network structure by interaction with selenite ions. The band at $\sim 500\,cm^{-1}$ shows no major changes. However, changes are observed to a large extent for the bands at ~ 600–$610\,cm^{-1}$, ~ 700–$720\,cm^{-1}$, and $860\,cm^{-1}$. The intensity of band at

$\sim$600–610 cm^{-1} increases as SeO$_2$ content increases, whereas that around 700–720 cm^{-1} diminishes. The band centered around 860–870 cm^{-1} shifts to higher wave number as SeO$_2$ content increases up to x = 0.50, but then decreases slightly as SeO$_2$ increases beyond x = 0.50. The band around 890 cm^{-1} shifts slightly towards lower wave number as SeO$_2$ content increases, indicating the vibration mode of isolated MoO$_6$ unit increases at higher SeO$_2$ content for highly modified glasses.

To quantify the relative proportion of different vibration modes present, the deconvolution of the FTIR spectra is performed. Here by deconvolution, respective area under different characteristic vibration modes is separated. The deconvoluted curves for a selected composition are shown in Fig. 1(c). From the determination of area under the curve for all the absorption bands, the relative area corresponding to absorption band is then calculated by dividing the respective area by total area under the curve. Fig. 2 shows the relative
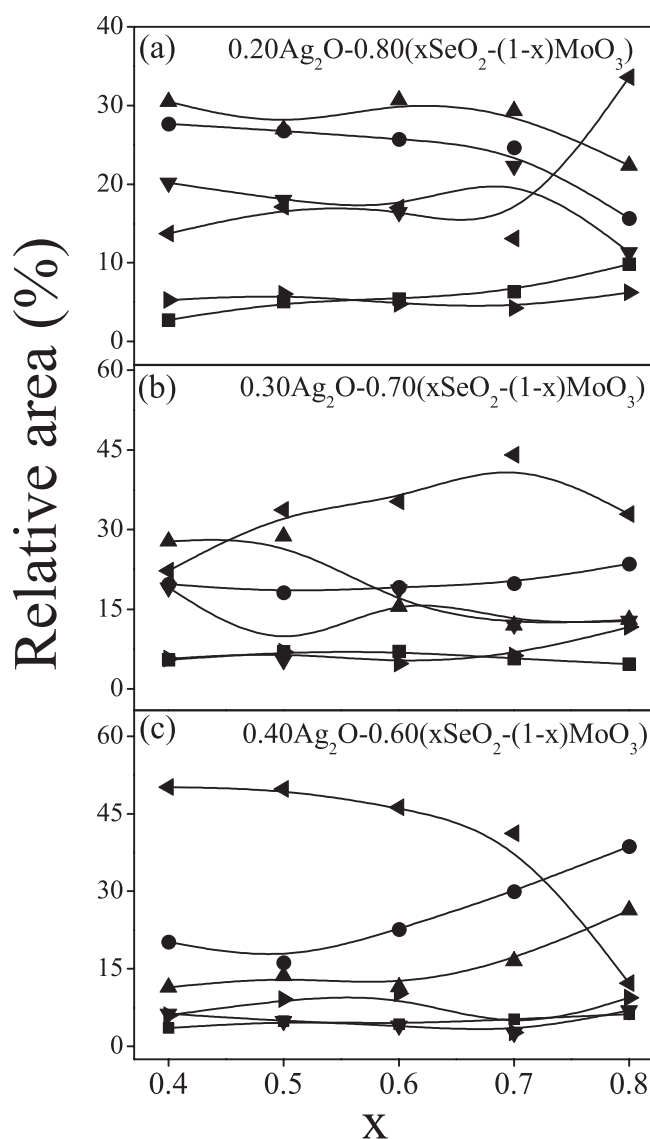
proportion of different vibration modes present in the glass compositions. The difference in the compositional dependency of the vibration modes can be easily observed in these figures.

For y = 0.20 series [see Fig. 2(a)], it is observed that the relative proportion of vibration bands for 500 cm^{-1} and 890 cm^{-1} is very low ($\sim$5%) and almost independent of composition. The relative proportion of vibration mode of band at 700–720 cm^{-1} and 760–780 cm^{-1} of SeO$_3^{2-}$ ion is quite high ($\sim$30%) and varies slightly with composition. The vibration mode at $\sim$860–870 cm^{-1} for SeO$_3^{2-}$ ion increases with increase of SeO$_2$ content, whereas vibration around 600 cm^{-1} decreases. For y = 0.30 series, the significant variation in the band proportion is observed for the 860–870 cm^{-1} and 600 cm^{-1} vibration modes. Thus, the relative proportion of 860–870 cm^{-1} and 600 cm^{-1} vibration mode is most significant, and their gradual change reflects the change in glass structure with composition. For y = 0.30 series [Fig. 2(b)], the mode of 860–870 cm^{-1} initially increases with increase of SeO$_2$ content similar to that of y = 0.20 series but decreases at higher SeO$_2$ content (x = 0.80). The band at 600 cm^{-1} decreases slightly as x increases up to 0.70 and then increases for x = 0.80 revealing a compositional dependency opposite to that of 860–870 cm^{-1} band. For y = 0.40 series [Fig. 2(c)], the variation of band is quite similar to that of y = 0.30 series but the vibration mode at 860–870 cm^{-1} decreases for x $\geq$ 0.60 and that of 600 cm^{-1} increases for x $\geq$ 0.60. It is further noted that the proportion of vibration mode around 860–870 cm^{-1} increases from $\sim$15% to almost $\sim$45%, whereas the relative proportion of 600 cm^{-1} decreases from $\sim$30% to $\sim$10% as y increases from 0.20 to 0.40 for x $\leq$ 0.70. From the above discussion, it is clear that the effect of gradual replacement of MoO$_3$ by SeO$_2$ causes the vibration of 860–870 cm^{-1} to increase while that of 600 cm^{-1} to decrease depending on modifier content (y). At high modifier and high SeO$_2$ content, a decrease in the vibration of 860–870 cm^{-1} and an increase of vibration mode at 600 cm^{-1} is observed. Thus at higher SeO$_2$ content, the vibration of SeO$_3^{2-}$ ion tends to decrease whereas that of isolated MoO$_6$ units increases and this might be due to the increased tendency of bonding of Ag$^+$ ions with SeO$_3^{2-}$ leading to the formation of Ag$_2$SeO$_3$ crystalline structure. The modification of glass network structure thus depends on glass formers ratio as well as on modifier to former ratio.

B. Dielectric constant

The complex dielectric permittivity $\varepsilon^*(f)$ can be expressed as

$$\varepsilon^*(f) = \varepsilon'(f) - i\varepsilon''(f), \qquad (1)$$

where $\varepsilon'(\omega)$ is the real part of $\varepsilon^*(f)$ known as dielectric constant and $\varepsilon''(f)$ is the imaginary part known as dielectric loss.[28] The frequency dependence of dielectric constant $\varepsilon'(f)$ for a selected composition at several temperatures is shown in Fig. 3(a). Fig. 3(b) shows the same for different compositions at a particular temperature. It is observed that $\varepsilon'(f)$ decreases with increase of frequency. The dielectric

FIG. 2. Variation of relative proportion of different vibration modes with composition for the glasses of composition yAg$_2$O-(1-y)(xSeO$_2$-(1-x)MoO$_3$) for band around (■) 500 cm^{-1}, (●) 600 cm^{-1}, (▲) 720 cm^{-1}, (▼) 760 cm^{-1}, (◄) 860 cm^{-1}, and (▶) 890 cm^{-1}. Solid lines are guide to the eye.
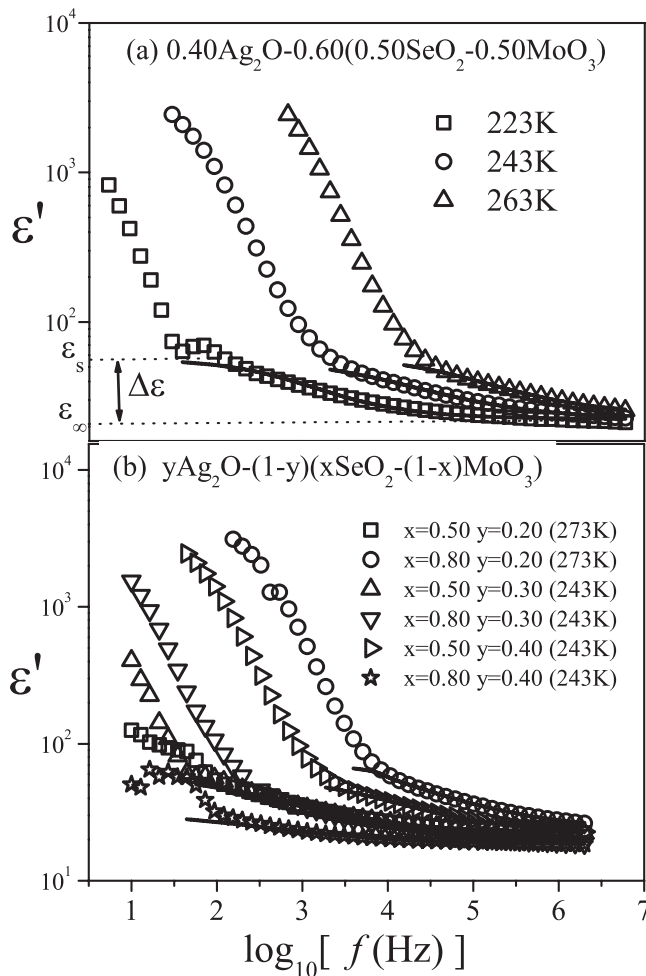
FIG. 3. (a) Variation of dielectric constant [$\varepsilon'(f)$] with frequency (f) for the glass composition 0.40Ag$_2$O-0.60(0.50SeO$_2$-0.50MoO$_3$) shown for several temperatures. (b) The same for several glasses of composition yAg$_2$O-(1-y)(xSeO$_2$-(1-x)MoO$_3$) for a fixed temperature. Solid lines are fits to Cole-Cole equation.

relaxation phenomena are usually associated with a frequency dependent orientational, interfacial, ionic, and dipolar polarization.[29] At low frequency, the permanent dipoles align themselves along the field and contribute fully to the total polarization of the dielectric. At higher frequency, the variation in the field is too rapid for the dipoles to align themselves, so their contribution to the polarization and hence, to dielectric permittivity can become negligible. Therefore, the dielectric permittivity, $\varepsilon'(f)$, decreases with increasing frequency.[30] From the frequency dependence of $\varepsilon'(f)$ [Fig. 3], it is observed that in the high frequency side, $\varepsilon'(f)$ shows a leveling-off and is denoted by ε_∞, which is attributed to the contribution from rapid polarization of atoms and electrons present in the samples under applied field.[28,31] In the intermediate frequency range, $\varepsilon'(f)$ increases with the decrease in frequency up to certain value, at which a plateau like feature is observed and the value at this level is denoted as ε_s. This may be related to the long range hoping motion of ions from one site to the others where polarization is associated with the changing environment of the different sites ions hops into.[28] It is observed that the onset of plateau shifts to higher frequency as the temperature is increased. It

is also noted that the value of $\varepsilon'(f)$ increases with the increase in temperature [Fig. 3(a)]. This can be understood from the temperature effect on dipolar, ionic, and electronic polarization. As the temperature increases, the orientation of dipoles is facilitated and consequently causes the dielectric constant to increase. Furthermore, at low temperatures, the contribution of electronic and ionic components to the total polarizability will be small. As the temperature is increased, sources of the electronic and ionic polarizability start to increase. The increase of $\varepsilon'(f)$ with increase of temperature thus may be linked to the increased dipolar polarization and the weakening of the intermolecular forces, which increases the orientational polarization and also to the increased contribution from ionic and electronic components to the polarizability. The electrode polarization comes into play at a frequency below which a steep increase in the value of $\varepsilon'(f)$ occurs as frequency decreases further. Thus at lower frequency, $\varepsilon'(f)$ increases rapidly by many orders of magnitude >10^4 which do not have a direct molecular interpretation but is a sign of the net impedance of the measured cell, where the contribution of the interface polarization to the total impedance is significant. The characteristics of bulk and electrode polarization can also be seen in the imaginary part of dielectric spectra. The $\varepsilon''(f)$ spectra for some selected compositions are shown in Figs. 4(a) and 4(b). The characteristics of the bulk sample and that of electrode polarization are clearly detected from this figure. It is observed that at higher frequency side as the frequency increases, the $\varepsilon''(f)$ gradually
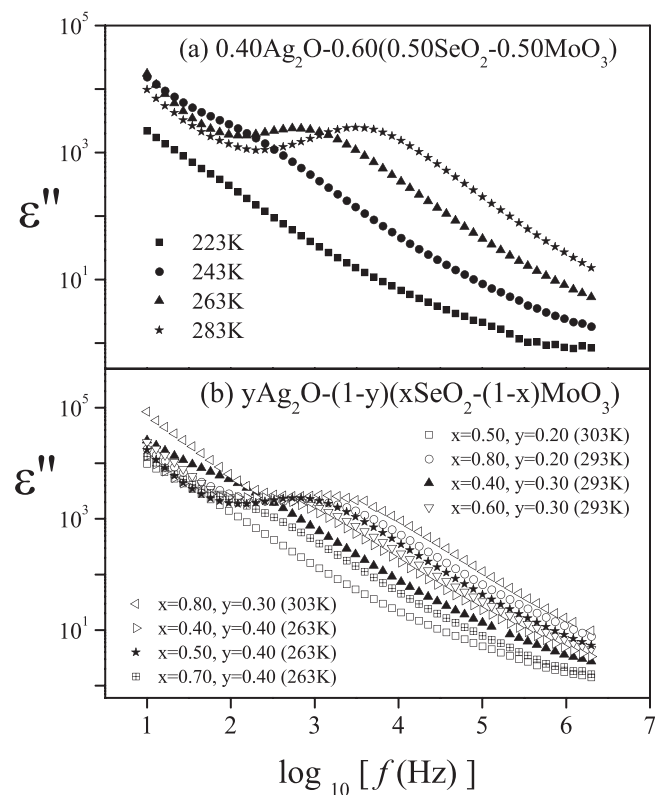

FIG. 4. (a) Variation of dielectric loss [$\varepsilon''(f)$] with frequency (f) for a glass composition 0.40Ag$_2$O-0.60(0.50SeO$_2$-0.50MoO$_3$) shown for several temperatures. (b) The same for several glasses of composition yAg$_2$O-(1-y)(xSeO$_2$-(1-x)MoO$_3$) for a fixed temperature.

decreases. As the frequency decreases, $\varepsilon''(f)$ value increases rapidly.

The study of dielectric constant data is invoked by using the Cole-Cole equation where the complex dielectric permittivity is expressed as[32]

$$\varepsilon^*(f) = \varepsilon_\infty + \frac{\varepsilon_s - \varepsilon_\infty}{1 + (i2\pi f \tau_{cc})^{1-\alpha}}, \qquad (2)$$

where τ_{cc} is the dielectric relaxation time and α is a measure of distribution of relaxation times with values $0 \leq \alpha < 1$. For an ideal Debye relaxation, $\alpha = 0$ and non-zero value of α will signify a distribution of relaxation times. The $\varepsilon''(f)$ is totally obscured by electrode polarization at lower frequency, so as to study the relaxation phenomenon we consider only $\varepsilon'(f)$ spectra to fit the Cole-Cole function given by Eq. (2). Now, the real part of $\varepsilon^*(f)$ is expressed as

$$\varepsilon'(f) = \varepsilon_\infty + \frac{(\varepsilon_s - \varepsilon_\infty)[1 + (2\pi f \tau_{cc})^{1-\alpha}\sin(\alpha\pi/2)]}{1 + 2(2\pi f \tau_{cc})^{1-\alpha}\sin(\alpha\pi/2) + (2\pi f \tau_{cc})^{2(1-\alpha)}}. \qquad (3)$$

Equation (3) is fitted to the experimental data for $\varepsilon'(f)$ as shown by solid lines in Figs. 3(a) and 3(b) neglecting lower frequency data that get obscured due to electrode polarization. The values of parameter such as ε_s, ε_∞, and α were determined from the fits. The values of these parameters for all the glasses are listed in Table I.

The compositional variation of ε' at a fixed frequency and temperature is shown in Fig 5(a). It is observed that for $y = 0.20$ series, the ε_s gradually increases with increase of SeO$_2$ content. For $y = 0.30$ and $y = 0.40$ series, the ε_s initially increases with increase of SeO$_2$ but decreases at higher SeO$_2$ content at $x = 0.80$ for $y = 0.30$ series and for $x \geq 0.60$ for $y = 0.40$ series. Fig. 5(b) shows the composition dependence of dielectric strength, $\Delta\varepsilon$ defined as the difference between
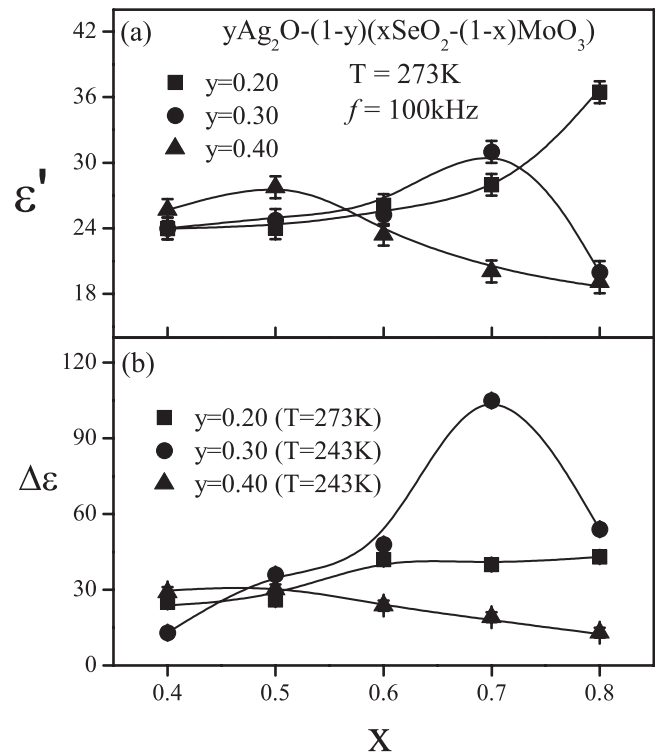

FIG. 5. Variation of (a) ε' at a fixed frequency and (b) $\Delta\varepsilon$ with SeO$_2$ content (x) for glasses of composition yAg$_2$O-(1-y)(xSeO$_2$-(1-x)MoO$_3$) shown for a fixed temperature. Solid lines are guide to the eye.

low frequency static value (ε_s) and the high frequency limiting value (ε_∞) of $\varepsilon'(f)$. It is noted in Fig. 5(b) that the compositional dependence of dielectric strength, $\Delta\varepsilon$ shows an increasing trend with increasing SeO$_2$ content for $y = 0.20$ series and shows maxima for $y = 0.30$ and 0.40 series similar to that observed for ε_s. The contribution to dielectric strength may be due to contribution from glass network formers and modifier as well as from different vibration modes of ions present in the glass structure. The increasing vibration of isolated SeO$_3^{2-}$ as ascertained from FTIR data directly correlates with the increase of dielectric constant and dielectric strength. The relative proportion of SeO$_3^{2-}$ ion increases with increase of SeO$_2$ content which is more polarizable compared to the isolated or bonded units. Thus, the dielectric constant as well as dielectric strength increases with the increase of free anions as SeO$_2$ content increases. However, for $x = 0.80$ for $y = 0.30$ series and for $x \geq 0.60$ for $y = 0.40$ series, the decrease of dielectric constant and strength could easily be understood from the increase of isolated molybdate units and for these glasses the possibility of bonding of selenite ions with Ag+ ions increases as revealed from FTIR data. This result signifies that the change of polarizable free anions within the glass matrix decreases, and thus the change of connectivity of network structure causes the dielectric constant and strength to change accordingly. This result also reveals the dual role of SeO$_2$ acting as a network modifier and a network former depending on composition. For $y = 0.30$ and 0.40 series, at lower SeO$_2$ content, the distortion of the network structure occurs as evident from the increased vibration of independent SeO$_3^{2-}$ ions, which indicates the decreasing glass forming ability of SeO$_2$ and

TABLE I. Compositional dependence of static dielectric constant ε_s, high frequency limiting dielectric constant (ε_∞), and Cole-Cole exponent α for the glass composition yAg$_2$O-(1 − y)(xSeO$_2$-(1 − x)MoO$_3$).

Composition	ε_s (± 1)	ε_∞ (± 1)	α (± 0.05)
y = 0.20			
x = 0.40	47 (273 K)	22 (273 K)	0.55 (303 K)
x = 0.50	48	22	0.56
x = 0.60	67	24	0.57
x = 0.70	62	22	0.56
x = 0.80	68	26	0.54
y = 0.30			
x = 0.40	36 (243 K)	23 (243 K)	0.49 (263 K)
x = 0.50	58	22	0.55
x = 0.60	70	22	0.53
x = 0.70	135	30	0.54
x = 0.80	71	17	0.46
y = 0.40			
x = 0.40	51 (243 K)	22 (243 K)	0.44 (243 K)
x = 0.50	53	23	0.42
x = 0.60	43	19	0.38
x = 0.70	38	19	0.40
x = 0.80	31	18	0.34

increasing modifier like behavior, whereas at higher SeO_2 content ($x = 0.80$ for $y = 0.30$ series and $x \geq 0.60$ for $y = 0.40$ series), the glass forming tendency of SeO_2 increases as for these compositions the vibration of independent SeO_3^{2-} ion decreases. For these glasses, the bonding of mobile $Ag+$ ions with SeO_3^{2-} ions is relatively high as gauged from the decrease of vibration of SeO_3^{2-} ions and increased vibration similar to that of isolated molybdate compounds.

For $y = 0.20$ series, the vibration of SeO_3^{2-} ions increases with increase of SeO_2 content (x) which signifies the modifier role of SeO_2 throughout the entire range of glass formation by creating more depolymerization or breaking of network structure. However, for $y = 0.30$ series, the vibration of SeO_3^{2-} ions increases initially up to $x \geq 0.70$, but, then increases for $x = 0.80$ which is attributed to the increased network forming tendency of SeO_2 as evident by the decrease of the SeO_3^{2-} vibration which bonds with free $Ag+$ ions to form silver selenite and also the vibration of isolated molybdate compounds increases at this composition. Similar arguments also hold for $y = 0.40$ series where a maximum in the composition dependence of the dielectric constant is observed. Here, the decrease at high SeO_2 content ($x \geq 0.60$) is attributed to the increased vibration of isolated MoO_6 units and decrease of independent SeO_3^{2-} ion vibration revealing the glass forming role of SeO_2 for these compositions.

IV. CONCLUSIONS

A correlation of structural and dielectric properties for the glass system Ag_2O-SeO_2-MoO_3 is presented. The existence of different absorption bands corresponding to the vibration of SeO_3^{2-} anions, isolated MoO_6 units, and molybdate octahedral units is ascertained from the FTIR study. It is observed that gradual replacement of MoO_3 by SeO_2 leads to the modification of the glass network structure, revealing the dual role of SeO_2 as either a modifier or a former depending on composition. The dielectric constant and dielectric strength of these glasses depend on the modification of glass structure and are strongly dependent on the change of relative proportion of SeO_3^{2-} vibration modes. The increase in dielectric relaxation strength for weakly modified glasses (0.20 and 0.30 mol fraction of Ag_2O) is related to the increase of the depolymerization of glass network related to the increased vibration of independent SeO_3^{2-} ions, signifying the modifier role of SeO_2, whereas the decrease for highly modified (0.40 mol fraction of Ag_2O) glasses are related to former like behavior of SeO_2 indicated by the decrease of the independent SeO_3^{2-} vibration and increased vibration of isolated molybdate compounds.

ACKNOWLEDGMENTS

[1]R. Prasada Rao, T. D. Tho, and S. Adams, J. Power Sources **189**, 385 (2009).

[2]B. Muthuraaman, S. Murugesan, V. Mathew, S. Ganesan, B. J. Paul, J. Madhavan, P. Maruthamuthu, and S. A. Suthanthiraraj, Sol. Energy Mater. Sol. Cells **92**, 1712 (2008).

[3]M. Abdel-Baki, A. M. Salem, F. A. Abdel-Wahab, and F. El-Diasty, J. Non-Cryst. Solids **354**, 4527 (2008).

[4]S. Murugesan, S. A. Suthanthiraraj, and P. Maruthamuthu, Mater. Res. Bull. **42**, 2017 (2007).

[5]P. Boolchand and W. J. Bresser, Nature (London) **410**, 1070 (2001).

[6]J. Swenson, R. L. McGreevy, L. Börjesson, and J. D. Wicks, Solid State Ionics **105**, 55 (1998).

[7]Y. Ogiwara, K. Echigo, and M. Hanaya, J. Non-Cryst. Solids **352**, 5192 (2006).

[8]J. Habasaki, J. Non-Cryst. Solids **353**, 3956 (2007).

[9]J. C. Dyre, P. Maass, B. Roling, and D. L. Sidebottom, Rep. Prog. Phys. **72**, 046501 (2009).

[10]J. L. Nowinski, M. Mroczkowska, J. R. Dygas, J. E. Garbarczyk, and M. Wasiucionek, Solid State Ionics **176**, 1775 (2005).

[11]S. S. Das, N. P. Singh, and P. K. Srivastava, Prog. Cryst. Growth Charact. Mater. **55**, 47 (2009).

[12]M. Foltyn, M. Wasiucionek, J. E. Garbarczyk, J. L. Nowinski, S. Gierlotka, and B. Palosz, J. Power Sources **173**, 795 (2007).

[13]B. Deb and A. Ghosh, J. Alloys Compd. **509**, 8251 (2011); Europhys. Lett. **97**, 16001 (2012); S. Kabi and A. Ghosh, Solid State Ionics **187**, 39 (2011).

[14]F. H. ElBatal, S. Y. Marzouk, and F. M. Ezz-ElDin, J. Mol. Struct. **986**, 22 (2011).

[15]Y. Dimitriev, I. Ivanova, V. Dimitrov, and L. Lackov, J. Mater. Sci. **21**, 142 (1986).

[16]S. Mandal and A. Ghosh, J. Phys.: Condens. Matter **8**, 829 (1996); M. T. Rinke and H. Eckert, Phys. Chem. Chem. Phys. **13**, 6552 (2011).

[17]C. C. de Araujo, W. Strojek, L. Zhang, H. Eckert, G. Poirier, S. J. L. Ribeiro, and Y. Messaddeq, J. Mater. Chem. **16**, 3277 (2006).

[18]S. M. Salem and E. A. Mohamed, J. Non-Cryst. Solids **357**, 1153 (2011).

[19]B. Vijaya Kumar, T. Sankarappa, S. Kumar, M. Prashant Kumar, P. J. Sadashivaiah, and R. R. Reddy, Physica B **404**, 3487 (2009).

[20]P. Limkitjaroenporn, J. Kaewkhao, P. Limsuwan, and W. Chewpraditkul, J. Phys. Chem. Solids **72**, 245 (2011).

[21]Y. Dimitriev, S. Yordanov, and L. Lakov, J. Non-Cryst. Solids **293–295**, 410 (2001).

[22]Y. Dimitriev, A. Bachvarova-Nedelcheva, and R. Iordanova, Mater. Res. Bull. **43**, 1905 (2008).

[23]A. Bachvarova, Y. Dimitriev, and R. Iordanova, J. Non-Cryst. Solids **351**, 998 (2005).

[24]C. H. Lee, K. H. Joo, J. H. Kim, S. G. Woo, H. J. Sohn, T. Kang, Y. Park, and J. Y. Oh, Solid State Ionics **149**, 59 (2002).

[25]C.-H. Lee, H.-J. Sohn, and M. G. Kim, Solid State Ionics **176**, 1237 (2005).

[26]M. Wübbenhorst, J. V. Turnhout, J. Non-Cryst. Solids **305**, 40 (2002).

[27]R. Iordanova, L. Aleksandrov, A. Bachvarova-Nedelcheva, M. AtaaLa, and Y. Dimitriev, J. Non-Cryst. Solids **357**, 2663 (2011).

[28]D. L. Sidebottom, Rev. Mod. Phys. **81**, 999 (2009).

[29]A. K. Jonscher, Dielectric Relaxation in Solids (Chelsea Dielectric, London, 1983).

[30]B. Deb and A. Ghosh, J. Appl. Phys. **108**, 074104 (2010); A. Ghosh, J. Appl. Phys. **65**, 227 (1989); A. Dutta and A. Ghosh, Phys. Rev. B **72**, 024201 (2005).

[31]A. Santic, C. W. Kim, D. E. Day, and A. Mogus-Milankovic, J. Non-Cryst. Solids **356**, 2699 (2010).

[32]K. S. Cole and R. H. Cole, J. Chem. Phys. **9**, 341 (1941).